Toxicology Letters 294 (2018) 193–204

Contents lists available at ScienceDirect

Toxicology Letters

journal homepage: www.elsevier.com/locate/toxlet

Peak AAA fatty acid homolog contaminants present in the dietary supplement L-Tryptophan associated with the onset of eosinophilia-myalgia syndrome

Klaus Klarskov[a], Hugo Gagnon[b], Mathieu Racine[b], Pierre-Luc Boudreault[c], Chad Normandin[c], Eric Marsault[c], Gerald J. Gleich[d], Stephen Naylor[e,*]

[a] Laboratory of Mass Spectrometry and Xenobiotics, Department of Pharmacology and Physiology, Faculty of Medicine and Health Sciences, Université de Sherbrooke, Sherbrooke, Québec, J1H 5N4, Canada
[b] PhenoSwitch Bioscience, Sherbrooke, Quebec J1H 5N4, Canada
[c] Department of Pharmacology and Physiology, Faculty of Medicine and Health Sciences, Université de Sherbrooke, Sherbrooke, Québec, J1H 5N4, Canada
[d] Departments of Dermatology and Medicine, School of Medicine, University of Utah, Salt Lake City, UT, 84132, USA
[e] ReNeuroGen LLC, Milwaukee, WI, 53122, USA

ARTICLE INFO

Keywords:
L-Tryptophan
Eosinophilia-myalgia syndrome
peak AAA
Case-associated contaminants
Dietary supplements
Structural homologs
Toxic oil syndrome

ABSTRACT

The eosinophilia-myalgia syndrome (EMS) outbreak that occurred in the USA and elsewhere in 1989 was caused by the ingestion of Showa Denko K.K. (SD) *L*-tryptophan (L-Trp). "Six compounds" detected in the L-Trp were reported as case-associated contaminants. Recently the final and most statistically significant contaminant, "Peak AAA" was structurally characterized. The "compound" was actually shown to be two structural isomers resulting from condensation reactions of L-Trp with fatty acids derived from the bacterial cell membrane. They were identified as the indole C-2 *anteiso* (AAA_1-343) and *linear* (AAA_2-343) aliphatic chain isomers. Based on those findings, we utilized a combination of on-line HPLC-electrospray ionization mass spectrometry (LC–MS), as well as both precursor and product ion tandem mass spectrometry (MS/MS) to facilitate identification of a homologous family of condensation products related to AAA_1-343 and AAA_2-343. We structurally characterized eight new AAA_1-XXX/AAA_2-XXX contaminants, where XXX represents the integer molecular ions of all the related homologs, differing by aliphatic chain length and isomer configuration. The contaminants were derived from the following fatty acids of the bacterial cell membrane, 5-methylheptanoic acid (*anteiso*-C8:0) for AAA_1-315; *n*-octanoic acid (*n*-C8:0) for AAA_2-315; 6-methyloctanoic acid (*anteiso*-C9:0) for AAA_1-329; *n*-nonanoic acid (n-C9:0) for AAA_2-329; 10-methyldodecanoic acid (*anteiso*-C13:0) for AAA_1-385; *n*-tridecanoic acid (*n*-C13:0) for AAA_2-385; 11-methyltridecanoic acid (*anteiso*-C14:0) for AAA_1-399; and *n*-tetradecanoic acid (*n*-C14:0) for AAA_2-399. The concentration levels for these contaminants were estimated to be 0.1–7.9 µg / 500 mg of an individual SD L-Trp tablet or capsule The structural similarity of these homologs to case-related contaminants of Spanish Toxic Oil Syndrome (TOS) is discussed.

1. Introduction

In late 1989 the USA Food and Drug Administration (FDA) issued a nationwide alert that advised consumers to stop consumption of manufactured *L*-Tryptophan (L-Trp) food products. The FDA also requested a recall of all L-Trp dietary supplements sold over-the counter. The resultant cause of such precipitous action was an outbreak of what became known as eosinophilia-myalgia syndrome (EMS) (Belongia et al., 1990; Belongia, 2004; Eidson et al. 1990; Kilbourne, 1992; Swygert et al., 1990;). EMS is a chronic, multisystemic disorder characterized by peripheral eosinophilia and sub-acute onset myalgia (Hertzman et al., 2001; Martin et al., 1990). In the aftermath over 1500

Abbreviations: AAA_1-XXX, all fatty acid homologs of AAA_1 family; AAA_2-XXX, all fatty acid homologs of AAA_2 family; CDC, USA centers for disease control and prevention; CE, collision energy; CES, collision energy spread; CID, collision induced dissociation; DoU, degree(s) of unsaturation; ESI, electrospray ionization; EMS, eosinophilia-myalgia syndrome; FDA, USA food and drug administration; HPLC, high performance liquid chromatography; IDA, information-dependent acquisition; LC–MS, microcapillary HPLC-mass spectrometry; LC-UV, HPLC with UV detection; L-Trp, *L*-tryptophan; MS/MS, tandem mass spectrometry; MS^n, multi-stage mass spectrometry; NMR, nuclear magnetic resonance; O-PAP, 1-Oleyl ester of PAP; OO-PAP, 1,2-Di-Oleyl ester of PAP; PAA, 3-(phenylamino)alanine; PAP, 3-(phenylamino)-1,2-propanediol; SD, showa denko K.K; TOF, time-of-fligh$_t$; TOS, toxic oil syndrome

* Corresponding author.
E-mail address: snaylor@rngen.com (S. Naylor).

https://doi.org/10.1016/j.toxlet.2018.05.027
Received 14 December 2017; Received in revised form 8 May 2018; Accepted 22 May 2018
Available online 22 May 2018
0378-4274/ © 2018 Elsevier B.V. All rights reserved.

patients were afflicted with EMS, and 38 deaths were directly attributed to the consumption of L-Trp in the USA alone (Swygert et al., 1993). Numerous other EMS cases were reported in Canada, UK, Germany, Belgium, France, Israel and Japan (Hertzman et al., 1991; COT-UK, 2004). In subsequent analyses by individual USA State health departments, and the US Centers for Disease Control and Prevention (CDC), it appeared that EMS was triggered by the consumption of the dietary supplement, L-Trp. Further investigation indicated that L-Trp produced by a single company, Showa Denko K.K. (SD) of Japan was primarily responsible for the EMS outbreak (Belongia et al., 1990; Slutsker et al., 1990).

The SD L-Trp was manufactured by a fermentation process that used a genetically engineered strain of *Bacillus amyloliquefaciens* (Belongia et al., 1992; Mayeno and Gleich, 1994). The epidemic was essentially curtailed when the FDA removed the suspect L-Trp from the retail market. Analyses of the SD L-Trp by high performance liquid chromatography (HPLC) and HPLC coupled on-line with mass spectrometry (LC–MS) revealed the presence of over sixty contaminants (Toyo'oka et al., 1991; Trucksess, 1993; Williamson et al., 1997, 1998a). Careful and exhaustive epidemiological studies as well as sample lot analyses of contaminated SD L-Trp determined that six contaminants were case-associated with the onset of EMS. These case-associated contaminants were identified as Peaks UV-5, E, 200, C, FF and AAA and named/labeled as a function of their unique HPLC retention times (Hill et al., 1993; Philen et al., 1993).

Structural characterization of all "six" case associated contaminants in SD L-Trp has now been completed. Peak UV-5 was identified as 3-(phenylamino)alanine (PAA) (Goda et al.,1992; Mayeno et al.,1992). Peak E was determined to be an acetaldehyde-tryptophan condensation reaction product, namely 1, 1' ethylidenebis(tryptophan) using a combination of MS, tandem mass spectrometry (MS/MS), nuclear magnetic resonance (NMR), and synthetic organic chemistry (Mayeno et al., 1990; Smith et al., 1991). Peak 200 was identified as 2-(3-indolylmethyl)-tryptophan using both NMR (Muller et al., 1991), and a combination of LC–MS and LC–MS/MS (Williamson et al., 1997). Peak C was determined by accurate mass LC–MS, LC–MS/MS and multistage mass spectrometry (MS^n) to be 3a-hydroxy-1,2,3,3a,8,8a-hexahydropyrrolo-[2,3-b]-indole-2-carboxylic acid (Williamson et al., 1998b). Peak FF was also subjected to the same analytical protocols as Peak C and identified as 2-(2-hydroxy indoline)-tryptophan (Williamson et al., 1998b). Recently we reported the structure determination of "Peak AAA", which Hill and coworkers had described as the most statistically significant contaminant in terms of association with EMS cases (Hill et al., 1993; Philen et al., 1993). This contaminant was determined to be actually two different fatty acid derived structural isomers. The structural isomers were identified as AAA_1-343 (*S*)-2-amino-3-(2-((*S,E*)-7-methylnon-1-en-1-yl)-1*H*-indol-3-yl)propanoic acid, and AAA_2-343 (*S*)-2-amino-3-(2-((*E*)-dec-1-en-1-yl)-1*H*-indol-3-yl)propanoic acid (Klarskov et al., 2018).

The efforts to determine causal onset of EMS have focused primarily on the structure determination of SD L-Tryptophan case-associated contaminants. However, there have been alternative suggestions as to the cause of EMS. Noakes and colleagues have argued that Quinolinic Acid may play a role in "cutaneous eosinophilic disorders" and hence by association EMS (Noakes et al., 2006). Others have argued that high doses of L-Trp alone were potentially responsible for EMS onset (Gross et al., 1999; Smith and Garrett, 2005). However, it is difficult to reconcile these findings with the original epidemiological work (Belongia et al., 1990; Slutsker et al., 1990; Swygert et al., 1993) and the subsequent analytical work and conclusions of Hill and Philen on SD L-Trp (Hill et al., 1993; Philen et al., 1993). We have argued that all the current EMS data in the literature supports the original consensus that the contaminants of SD L-Trp were responsible for the EMS outbreak (Naylor, 2017). This hypothesis is further reinforced by consideration of an earlier, disease related outbreak of Spanish Toxic Oil Syndrome (TOS).

The TOS outbreak was a related manifestation of elevated eosinophils associated with food and dietary supplement consumption that occurred in 1981 (Gelpi et al. 2002). TOS was caused by the ingestion of aniline-adulterated cooking oil, fraudulently sold by Spanish street-vendors as olive oil. The clinical symptoms manifested by TOS patients closely resembled those of EMS patients and were characterized by incapacitating myalgias and elevated peripheral eosinophils. The health impact was dramatic since in excess of 20,000 individuals were affected and over 300 deaths occurred in the first twenty months of the TOS epidemic. It was further estimated that an additional ~1690 premature deaths due to the use of the tainted oil occurred during the time period 1983–1997 (Gelpi et al., 2002).

In the present work we report the structure identification of a series of fatty acid condensation product homologs produced during the fermentation process. They are derived from the reaction of SD L-Trp with the *Bacillus amyloliquefaciens* lipid membrane fatty acids. We quantify all ten AAA_1-XXX/AAA_2-XXX contaminants present in the SD L-Trp ingested by patients at the time of the epidemic. Note that "XXX" represents the integer molecular ions of all the related homologs, differing by aliphatic chain length and isomer configuration. Finally, we discuss the structural similarities of these new contaminants with those of case-related contaminants from toxic oil shown to cause TOS.

2. Materials and methods

2.1. Chemicals and reagents

LC–MS grade water, methanol and acetonitrile were purchased from Millipore-Canada Ltd (Etobicoke, ON, Canada). Formic acid and L-Trp were obtained from either Sigma (Markham, ON, Canada) or Millipore-Canada. The synthesis and structural characterization of the standard *anteiso* AAA_1-343 is described in detail elsewhere (Klarskov et al., 2018). Solid phase Sep-Pak™ C-18 cartridges were obtained from Waters Corporation (Mississauga, ON, Canada).

2.2. Showa Denko L-Trp

Dr. Rossanne Philen (CDC) provided SD case-implicated L-Trp. This sample lot was manufactured between January-June 1989, and had previously been demonstrated as case-implicated in EMS onset (Hill et al., 1993; Mayeno and Gleich, 1994; Philen et al., 1993). Sample storage and handling at the CDC has been described elsewhere (Hill et al., 1993; Philen et al., 1993). We received these samples on September 10th, 1996. All samples were kept in Fisher Scientific polypropylene centrifuge tubes with screw caps, under Nitrogen and further sealed with parafilm. These sample tubes were kept either at room temperature or at −20 °C in assorted commercial freezers and out of contact with direct light except in brief instances of sample handling and preparation for analyses. In the case of sample analyses, all samples were prepared fresh on each occasion as described in section 2.3 below.

2.2.1. Composition and stability of SD L-Trp

The L-Trp sample lots originally analyzed by Hill and Philen were provided by SD and were manufactured between January 1987, and November 1989 (Hill et al., 1993; Philen et al., 1993). Dr. Philen (CDC) provided one such sample lot to us. Our sample is now almost thirty years old. However, we have regularly evaluated the sample integrity and stability. The CDC performed the initial HPLC analysis of the sample in 1993 and they published a HPLC UV chromatogram complete with an internal standard (Hill et al., 1993). In the intervening years we have evaluated the same sample using similar HPLC conditions with either simple UV detection (Williamson et al., 1998a) or MS (Mayeno et al., 1995) and MS/MS detection (Klarskov et al., 2000, 2018; Williamson et al., 1997; Williamson et al., 1998b). In all cases the relative composition of the chromatogram has not discernibly changed based on the number of peaks detected or the relative peak intensities

determined either by UV or MS and MS/MS.

2.3. L-Trp sample extraction

SD case-implicated L-Trp was dissolved in 50% aqueous methanol to a concentration of 20 mg/mL. Following sonication for 30 min each sample was centrifuged at 13,000 rpm using a Heraeus Biofuge (Fisher Scientific, Canada). The supernatant was diluted 10x in water and loaded onto a methanol pre-equilibrated and water rinsed C_{18} solid phase cartridge. After an initial rinsing of the cartridge with 5% (v/v) aqueous methanol, L-Trp contaminants were eluted with 0.5 mL of methanol and vacuum dried. The samples were dissolved in 100 µL 50% (v/v) aqueous acetonitrile containing 0.2% (v/v) formic acid prior to LC–MS/MS analysis.

2.4. Mass spectrometry of SD L-Trp

2.4.1. LC–MS and LC–MS/MS

Separations were done online using an Eksigent micro-UHPLC 200 (Sciex, California, US). Individual samples were injected onto a Polar C-18 reversed phase Luna Omega column, 50 x 1 mm ID, with a 1.6 µm particle size (Phenomenex, CA, US) by loop overfilling using a 5 µL injection loop. A LC gradient consisting of 0.2% (v/v) aqueous formic acid in water as Phase A, and methanol with 0.2% formic acid as Phase B at a flow rate of 60 µL/min. was used with following gradient conditions: (%B/min) 60/0, 60/0.2, 100/5.6, 100/6.3, 40/6.4 40/7. All LC–MS and LC–MS/MS analyses were done in positive mode on a Triple Tine-of-Flight (TOF) 5600 (Sciex, California, US) equipped with an electrospray ion source. High resolution TOF-MS survey scans were set for each precursor ion as follows: 315.2 (*m/z* 290–330, 20 ms/scan), 329.2 (*m/z* 300–340, 20 ms/scan), 343.2 (*m/z* 320–370, 20 ms/scan), 385.2 (*m/z* 350–400, 50 ms/scan) and 399.2 (*m/z* 370–430, 50 ms/scan) were followed by a series of product ion scans (0.7 Da Q1 precursor window) with collision energy (CE) adjusted to each product ion (315, 329, 343 (CID 35 V), 385 and 399 (CID 45 V)) with a collision energy spread (CES) of 20. The total cycle time was 385 ms. Curtain, ion source 1 and 2 gas were respectively 28, 14 and 17 L/min.

2.4.2. LC–MS and LC–MS/MS quantification of AAA_1-XXX/AAA_2-XXX contaminants

Analytical conditions to carry out the quantification of all AAA_1-XXX and AAA_2-XXX contaminants present in Showa Denko L-Trp are described above in Section 2.4.1. A calibration curves were constructed using commercially available L-Trp in conjunction with synthetic *anteiso* AAA_1-343. Once the concentration of authentic AAA_1-343 in SD L-Trp was determined, we used the relative ion count-area under the curve method to determine the other concentration values of all the AAA_1-XXX and AAA_2-XXX contaminants present in SD L-Trp.

2.4.3. LC–MS/MS with information-dependent acquisition (IDA)

Separations were done as described above, except that samples were injected onto a C-18 reversed phase HALO column, 100 x 0.5 mm ID, 2.7 µm particle size, 90 Å pore size (Sciex, California, US). The LC gradient consisted of 0.1% (v/v) aqueous formic acid in water as Phase A, and acetonitrile with 0.1% formic acid as Phase B and a flow rate of 35 µL/min. was used with the following gradient: (%B/min) 5/0, 5/0.5, 90/2.3, 90/2.9, 5/3 5/3.5. Information-Dependent Acquisition (IDA) mode triggered five dependent MS/MS scans (*m/z* 50–600 with an accumulation time of 100 ms per scan) per precursor ion when the intensity of the latter was above 75 counts. Precursor ion LC–MS scans (*m/z* 200–600) were accumulated in 250 msec with a cycle time of 800 msec. MS/MS spectra that contained a *m/z* 168 product ion were selectively identified using the PeakView software (Sciex).

3. Results & discussion

"Peak AAA" was recently determined to be two structural isomers, namely AAA_1-343 and AAA_2-343. They were formed from condensation reactions of L-Trp with bacterial lipid membrane derived fatty acids (Klarskov et al., 2018). Simat has argued that the manufacturing process of SD L-Trp produced six different types of contaminants that included i. bacterial metabolites, ii. oxidation products, iii. carbonyl condensation compounds, iv. 2-substituted–Trp derivatives, v. 1-substitued-Trp derivatives and vi. PAA and related compounds (Simat et al., 1999). The structures AAA_1-343 and AAA_2-343 are representative of 2-substituted-Trp derivatives. The ingestion of such fatty acid derived aliphatic chain containing compounds, would have resulted in very different absorption, distribution, metabolism and excretion profiles of AAA_1-343 and AAA_2-343 through the body for a person consuming SD L-Trp. This may be of some relevance in ascertaining the causal onset of EMS. Hence, we were interested in determining if other fatty acid derived L-Trp condensation products were present in SD L-Trp.

The structure determination of AAA_1-343 and AAA_2-343 employed the use of accurate mass LC—MS/MS analysis. The resulting product ion spectra for both AAA_1-343 (Fig. 1a) and AAA_2-343 (Fig. 1b) revealed an unexpected, but prominent product ion at *m/z* 168. The relative abundance of this ion indicated a facile fragmentation process that produced a stable product ion. We have previously reported that LC-multistage tandem mass spectrometry (MS^n) of the ion at *m/z* 168 for AAA_1-343 and AAA_2-343 were identical, and subsequently compared against a number of MS and MS/MS spectral databases (Klarskov et al., 2018). The comparative search revealed that the product ion at *m/z* 168 was structurally similar to that of the aromatic heterocycle carbazole, as shown in the insert of Fig. 1a and b. (Oberacher, 2013; Klarskov et al., 2018). The presence of this product at *m/z* 168 and its structural identification were crucial in determining that the fatty acid-derived aliphatic chain was attached at the C-2 carbon of the indole ring, and contained a double bond at the C1'-C2' position (Fig. 1a-b) (Klarskov et al., 2018).

3.1. Precursor ion MS/MS scans of L-Trp

As noted above the prominent product ion at *m/z* 168 is indicative of compounds derived from a condensation reaction of L-Trp with fatty acids from the *Bacillus amyloliquefaciens* lipid membrane. We used the presence of this ion in our MS/MS analyses as a vehicle to search for other possible homologs of AAA_1-343 and AAA_2-343. We performed an accurate mass precursor ion scan MS/MS analysis of the SD L-Trp extract. In this type of analysis all protonated molecular ions (MH^+) are subjected to fragmentation through CID. Following the analysis, MS/MS spectra that contain a specific fragment ion of interest, in this case *m/z* 168 can then be selectively plotted (Glish and Vachet, 2003). The resultant precursor ion MS/MS analysis (*m/z* 168) undertaken on SD L-Trp in IDA mode, exhibited a number of MH^+ species shown in Fig. 2.

Perusal of these data revealed the presence of an ion series at $MH^=$ = 315.2079; 329.2232; 343.2384; 385.2858 and 399.3011, all differing by multiples of 14 mass units. Since the precursor ion scan was done using accurate mass LC—MS/MS it was possible to determine the molecular formula and the Degree of Unsaturation (DoU) of each MH^+ ion. The ion at MH^+ = 343.2384, possesses a DoU = 8, and a molecular formula of $C_{21}H_{31}N_2O_2$ corresponding to the previously described AAA_1-343 fatty acid – L-Trp reaction product shown in Fig. 1a. The other four MH^+ ions share the same DoU but differ in their -C_nH_{2n}- composition (Table 1). These MH^+ species afford a product ion (*m/z* 168) that indicates the presence of an indole C-2 linkage with a double bond at the C1′-C2′ position, this suggests that they are fatty acid-L-Trp condensation products of differing aliphatic chain lengths. In specific terms, the ions at MH^+ of 315, 329, 385 and 399 may represent the presence of a homologous series of fatty acid condensation products

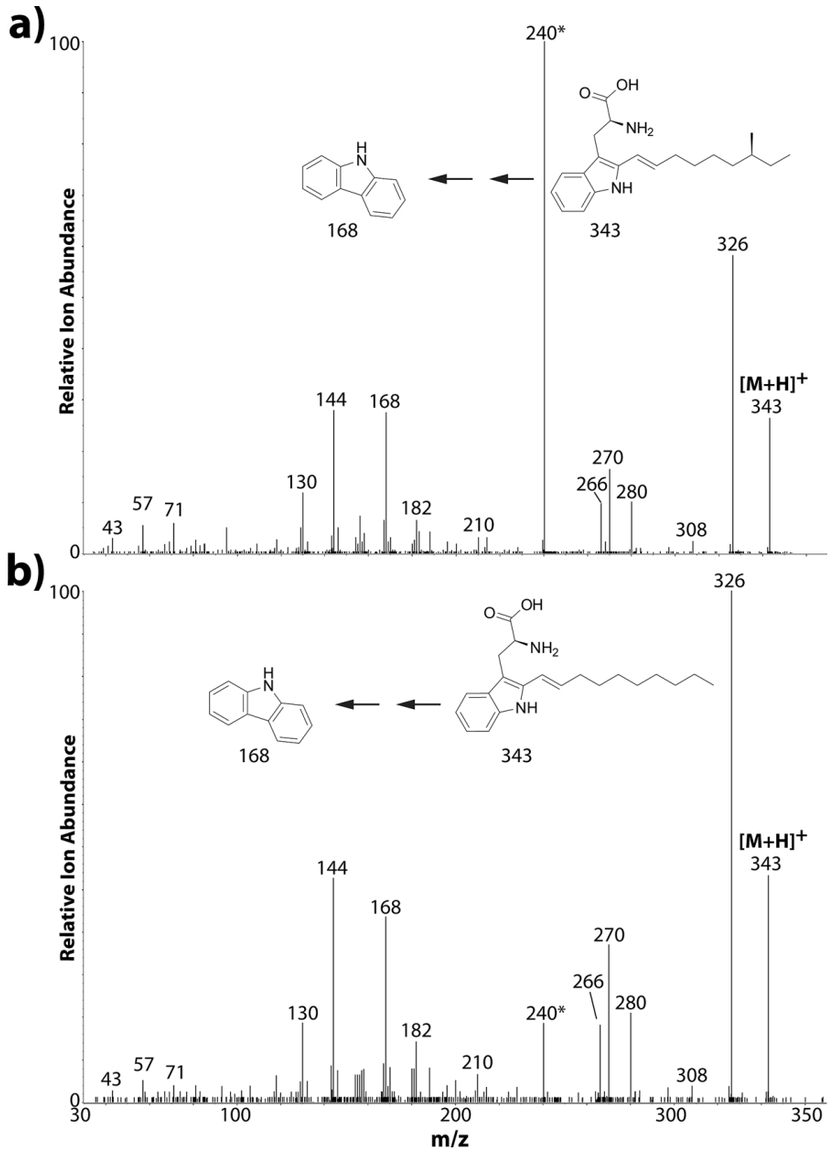

Fig. 1. Accurate mass LC–MS/MS of authentic AAA_1-343 and AAA_2-343 from SD L-Trp.
a. Product ion spectrum for AAA_1-343 derived from precursor ion MH^+ = 343.2386.
a. Product ion spectrum for AAA_2-343 derived from precursor ion MH^+ = 343.2386.
Integer product ion masses are shown for clarity, and the accurate mass values are contained in Table 1 and S1.
The insert shows the structures of AAA_1-343 and AAA_2-343 as well as the structure of the product ion (non-protonated form) at *m/z* 168.
* The product ion at *m/z* 240* is a contaminant derived from the LC column.

with L-Trp containing C_8, C_9, C_{13} and C_{14} aliphatic chain lengths respectively. Note that the MH^+ ions at *m/z* 277.1193 (DoU = 8; molecular formula $C_{14}H_{17}N_2O_4$) and *m/z* 329.1280 (DoU = 15; molecular formula $C_{21}H_{17}N_2O_{2)}$ denoted in red (Fig. 2) are other L-Tryptophan moieties. They are unrelated to the homologous fatty acid series derived L-Trp condensation products. This conclusion is based on their molecular formulae, DoU and MS/MS product ion spectra, (data not shown).

3.2. Survey scan LC–MS of AAA homologs

The precursor ion scan selection of *m/z* 168 described above (Fig. 2), only revealed one AAA_x-343 isomer. Taking into account our recent results demonstrating the presence of two isomers, indicated that this LC-MS/MS approach suffered limited HPLC resolution. We performed a survey scan LC–MS ion chromatogram analysis on SD L-Trp employing different HPLC conditions (see Section 2.4.1 above) and scanned for each precursor ion as follows: 315.2 (*m/z* 290–330), 329.2 (*m/z* 300–340), 343.2 (*m/z* 320–370), 385.2 (*m/z* 350–400) and 399.2 (*m/z* 370–430). The resultant survey-scan LC–MS ion chromatograms are shown in Fig. 3a-e. Each ion pair possesses individual ion components with identical protonated molecular ions (within experimental error).

The accurate mass MH^+ ions identified were 315.2073 (AAA_1-315), 315.2090 (AAA_2-315) (Fig. 3a), 329.2237 (AAA_1-329), 329.2232 (AAA_2-329) (Fig. 3b), 343.2386 (AAA_1-343), 343.2386 (AAA_2-343) (Fig. 3c), 385.2847 (AAA_1-385), 385.2841 (AAA_2-385) (Fig. 3d), as well as 399.2982 (AAA_1-399) and 399.3004 (AAA_2-399) (Fig. 3e). Based on the accurate mass data all these precursor ion species possessed a molecular formula of $C_nH_{(n+x)}N_2O_2$ (where x = 8, 9, 10, 13 or 14), and a DoU = 8 (see both Table 1 and Supplemental Table S1). The ion pair that afforded MH^+ = 343.2386 is the previously described AAA_1-343 and AAA_2-343 contaminants shown in Fig. 1a and b respectively. The four ion pairs AAA_1-315/AAA_2-315; AAA_1-329/AAA_2-329; AAA_1-385/AAA_2-385; and AAA_1-399/AAA_2-399 (hereafter referred to as AAA_1-XXX and/or AAA_2-XXX) all appear to be fatty acid homologs of L-Trp, and possibly contain *anteiso*, *iso* or *linear* aliphatic

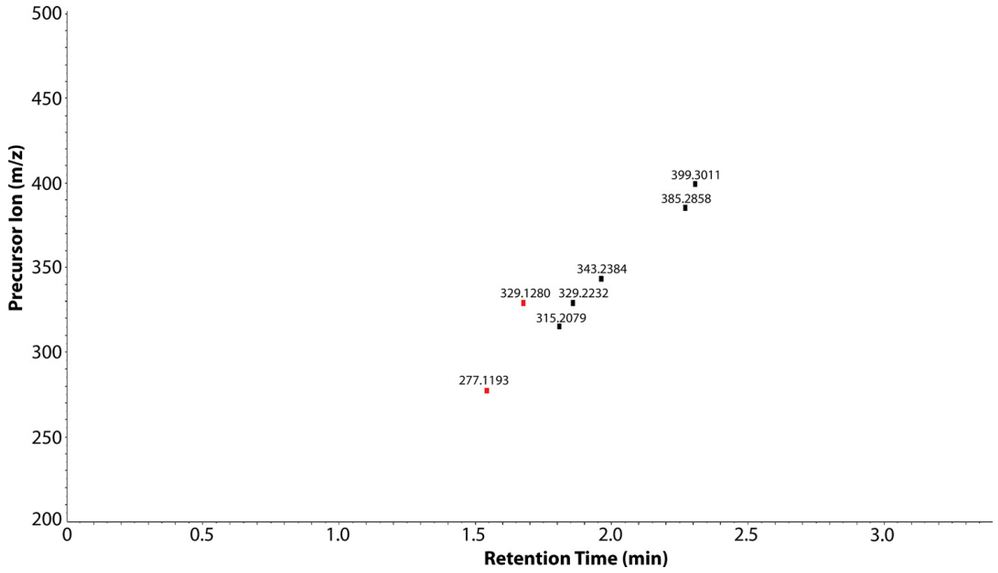

Fig. 2. Accurate mass LC–MS/MS of SD L-Trp with Information Dependent Acquisition (IDA) Mode. The precursor ion selected was m/z 168 (note on the Sciex 5600 this is done post-analysis).
Note that the ions denoted in red are not part of the homologous ion series, but other unrelated L-Tryptophan containing moieties.

chains as previously discussed for AAA_1-343 and AAA_2-343 (Klarskov et al., 2018).

3.3. LC–MS/MS product ion spectra of AAA homologs

In order to further elucidate the structures of the eight potential fatty acid homologs AAA_1-XXX and AAA_2-XXX compounds in the SD L-Trp, all selected precursor ions were subjected to very similar ionization and collision conditions employing accurate mass LC–MS/MS. These product ion spectra are shown in Fig. 4a-h. Since these data were acquired in accurate mass MS/MS mode, it was possible to determine both the molecular ion formula and DoU for all product ions shown in Fig. 4a-h. This is summarized in Table 1 for AAA_1-315, AAA_1-329, AAA_1-385, and AAA_1-399 as well as Table S1 for AAA_2-315, AAA_2-329, AAA_2-385, and AAA_2-399. The product ion spectra of all these contaminants are discussed in detail below.

3.3.1. Product ions from L-Trp amino-carboxylic acid side chain

The product ion spectra of both AAA_1-343 and AAA_2-343 contained identical ions at *m/z* 326, 308, 280 and 270 (Fig. 1a and b). They correspond to fragment ion losses of (MH^+- NH_3) (see Scheme 1,[**II**]), (MH^+- NH_3 - H_2O) (Scheme 1,[**III**]), (MH^+- NH_3 −HCOOH) (Scheme 1,[**IV**], and (MH^+ −HCN −HCOOH) (Scheme 1, [**V**]) respectively (El Aribi et al., 2004; Lioe et al., 2004; and Klarskov et al., 2018). Inspection of the product ion spectra of AAA_1-315/AAA_2-315 (*m/z* 298, 280, 252, 242); AAA_1-329/AAA_2-329 (*m/z* 312, 294, 266, 256); AAA_1-385/AAA_2-385 (*m/z* 368, 350, 322, 312) and AAA_1-399/AAA_2-399 (*m/z* 382, 364, 336, 326) revealed that the same fragment ion losses occur for all the contaminants (see Fig. 4a-h, and Table 1 and Table S1). These fragment ion losses and resulting product ion structures ([**II**], [**III**], [**IV**] and [**VI**]) are shown in Scheme 1 for all eight members of the AAA_1-XXX and AAA_2-XXX homologous family of contaminants. These ion series and the associated fragmentation losses clearly indicate that neither the L-Trp amino nor the carboxylic acid functional groups in AAA_1-XXX and AAA_2-XXX are modified.

3.3.2. Product ion series from the indole ring

The eight product ion spectra of the AAA_1-XXX and AAA_2-XXX

Table 1
Accurate mass MS/MS Product ion data for AAA_1 homologous series, namely AAA_1-315, AAA_1-329, AAA_1-343, AAA_1-385, and AAA_1-399.

Number in Scheme 1[a]	Measured Mass **AAA_1-315**	Measured Mass **AAA_1-329**	Measured Mass **AAA_1-343**	Measured Mass **AAA_1-385**	Measured Mass **AAA_1-399**	DoU[b]	Molecular Composition[c] **315/329/343/385/399**
Not Shown	43.0567	43.0556	43.0585	43.0570	43.0561	1[d]	**C**3**H**7
Not Shown	57.0721	57.0713	57.0737	57.0710	57.0711	1[d]	**C**4 **H**9
Not Shown	71.0865	71.0865	71.0883	71.0863	71.0860	1[d]	**C**5 **H**11
[**XII**$_a$]	118.0662	118.0656	118.0657	118.0659	118.0665	6	**C**8 **H**8 **N**
[**XI**[a]]	130.0651	130.0653	130.0660	130.0654	130.0659	7	**C**9 **H**8 **N**
[**IX**[a], **X**[a]]	144.0813	144.0813	144.0815	144.0813	144.0814	7	**C**10 **H**10 **N**
[**VIII**[a]]	168.0813	168.0813	168.0811	168.0813	168.0813	9	**C**12 **H**10 **N**
[**VII**[a]]	182.0963	182.0968	182.0964	182.0971	182.0973	9	**C**13 **H**12 **N**
[**VI**[a]]	238.1591	252.1750	266.1888	308.2378	322.2544	9	**C**17/18/19/22/23 **H**20/22/24/30/32 **N**
[**V**[a]]	242.1908	256.2066	270.2210	312.2689	326.2842	7	**C**17/18/19/22/23 **H**24/26/28/34/36 **N**
[**IV**[a]]	252.1743	266.1914	280.2048	322.2543	336.2702	9	**C**18/19/20/23/24 **H**22/24/26/32/34 **N**
[**III**[a]]	280.1736	294.1834	308.1993	350.2473	364.2638	10	**C**19/20/21/24/25 **H**22/24/26/32/34 **N O**
[**II**[a]]	298.1814	312.1969	326.2111	368.2587	382.2753	9	**C**19/20/21/24/25 **H**24/26/28/34/36 **N O**2
[**I**[a]]	315.2073	329.2237	343.2386	385.2847	399.2982	8	**C**19/20/21/24/25 **H**27/29/31/37/39 **N**2 **O**2

[a] See Scheme 1 for corresponding precursor or product ion structure.
[b] Degrees of Unsaturation (DoU) for the uncharged molecular species.
[c] Molecular Composition for the protonated charged ion species.
[d] These ions can either be protonated charged ion or radical cation ion species.

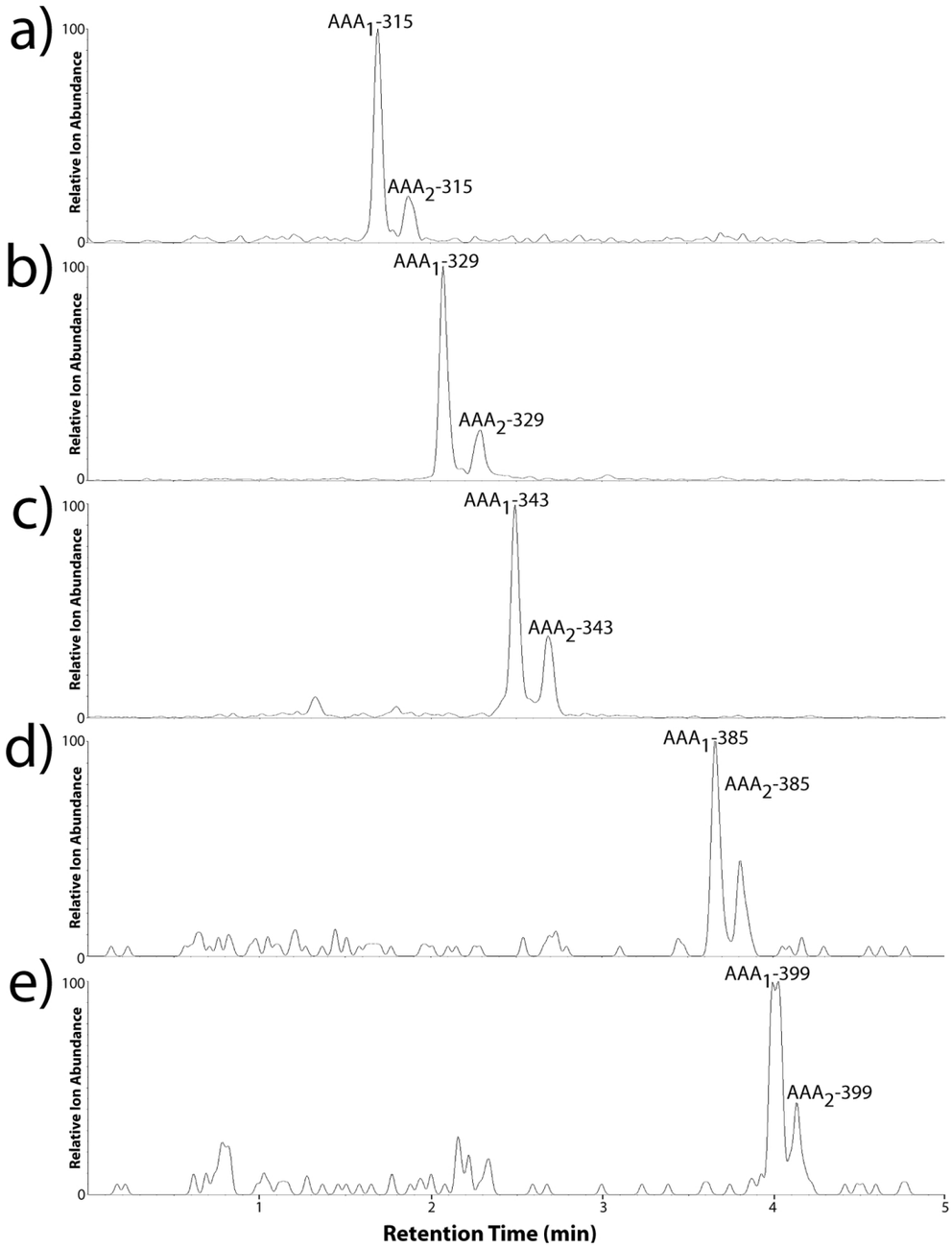

Fig. 3. Normalized precursor survey scan accurate mass LC–MS ion chromatogram of SD L-Trp.
a) *m/z* 315.2 (mass range scan *m/z* 290–330).
a) *m/z* 329.2 (mass range scan *m/z* 300–340).
a) *m/z* 343.2 (mass range scan *m/z* 320–370).
a) *m/z* 385.2 (mass range scan *m/z* 350–400).
a) *m/z* 399.2 (mass range scan *m/z* 370–430).

contaminants (Fig. 4a-h) as well as AAA_1-343 and AAA_2 -343 (Fig. 1a-b) all contained product ions at *m/z* 144 ([**IX**] and [**X**], Scheme 1), 130 ([**XI**], Scheme 1) and 118 ([**XII**], Scheme 1), and also see Table 1 and Table S1. These ions confirm the presence of an intact indole ring of L-Trp (El Aribi et al., 2004). This ion series also indicates that the benzene ring (C-4 through C-7) of the indole moiety has not been substituted for any of the AAA_1-XXX or AAA_2-XXX family of contaminants (see Scheme 1). In contrast, a MS/MS analysis of a substituted indole, e.g. 5-hydroxy-tryptophan, exhibited a product ion series at *m/z* 162, 146 and 134, reflecting the presence of a hydroxylated indole ring at C-5. (Williamson et al.,1998b).

3.3.3. Product ion at m/z 168, and related ion series

Analyses of both AAA_1 -343 and AAA_2-343 (Fig. 1a and b) and all eight AAA_1-XXX and AAA_2-XXX product ion spectra (Fig. 4a-h) revealed a prominent product ion at *m/z* 168. As discussed above, the relative abundance of this ion in all product ion spectra indicates a facile fragmentation process that produces a stable carbazole product ion (Scheme1,[**VIII**]). It is noteworthy that MS/MS spectra of AAA_1-343 and AAA_2-343 contain ions at *m/z* 266 and 182 (Fig. 1a and b; Table 1 and S1) structurally related to *m/z* 168. Multistage tandem MS (MS^n) analyses of the *m/z* 266 and 182 ions both afforded the carbazole ion at *m/z* 168 (Klarskov et al., 2018).

Analysis of the product ion spectra of AAA_1-315/AAA_2-315 (*m/z* 238 and 182); AAA_1-329/AAA_2-329 (*m/z* 252 and 182); AAA_1-385/

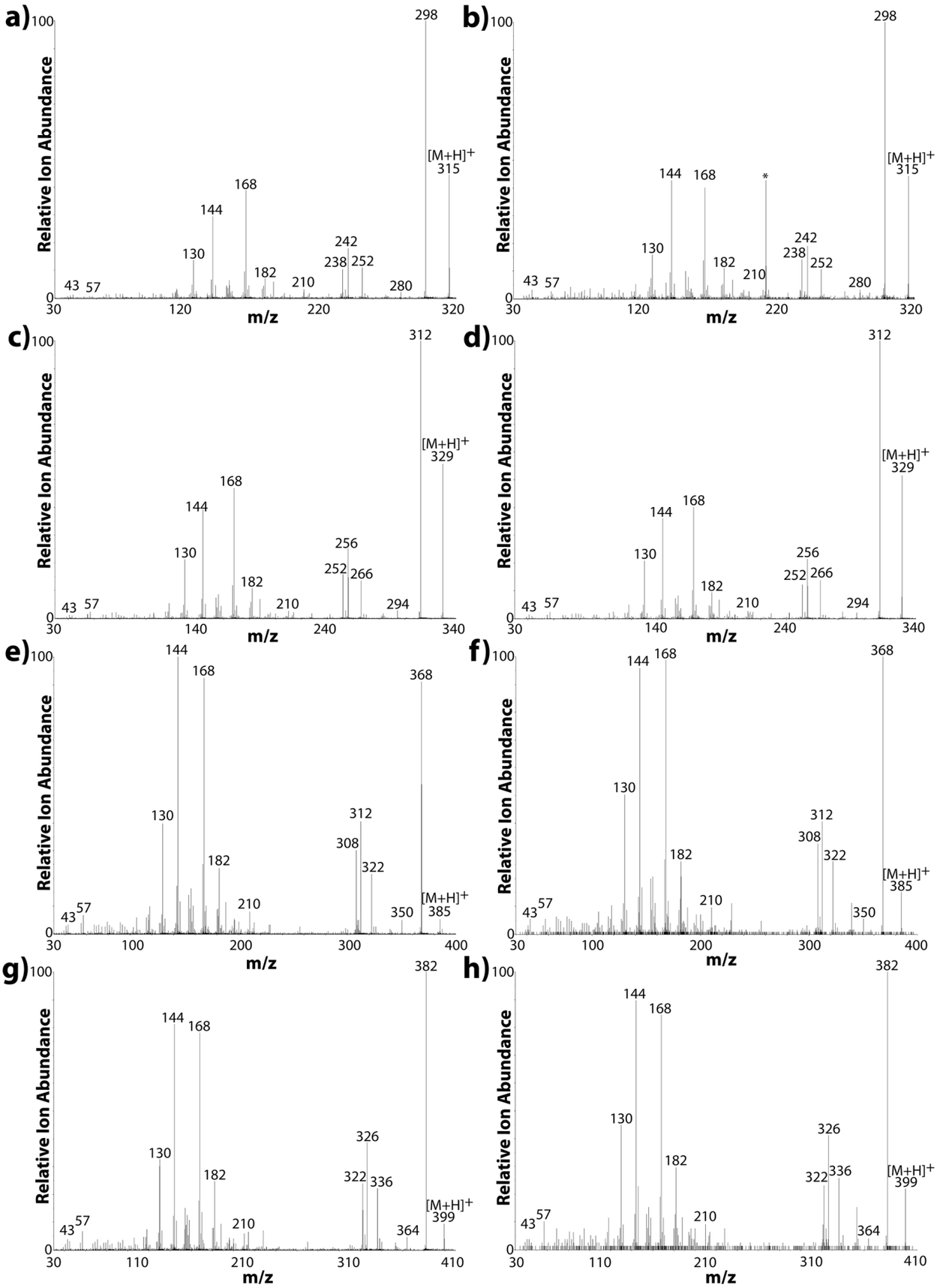

Fig. 4. Product ion accurate mass LC–MS/MS spectra of SD L-Trp.
a) AAA_1-315; b) AAA_2-315.
c) AAA_1-329; d) AAA_2-329.
e) AAA_1-385; f) AAA_2-385.
g) AAA_1-399; h) AAA_2-399.
* This product ion is a contaminant derived from the LC column.

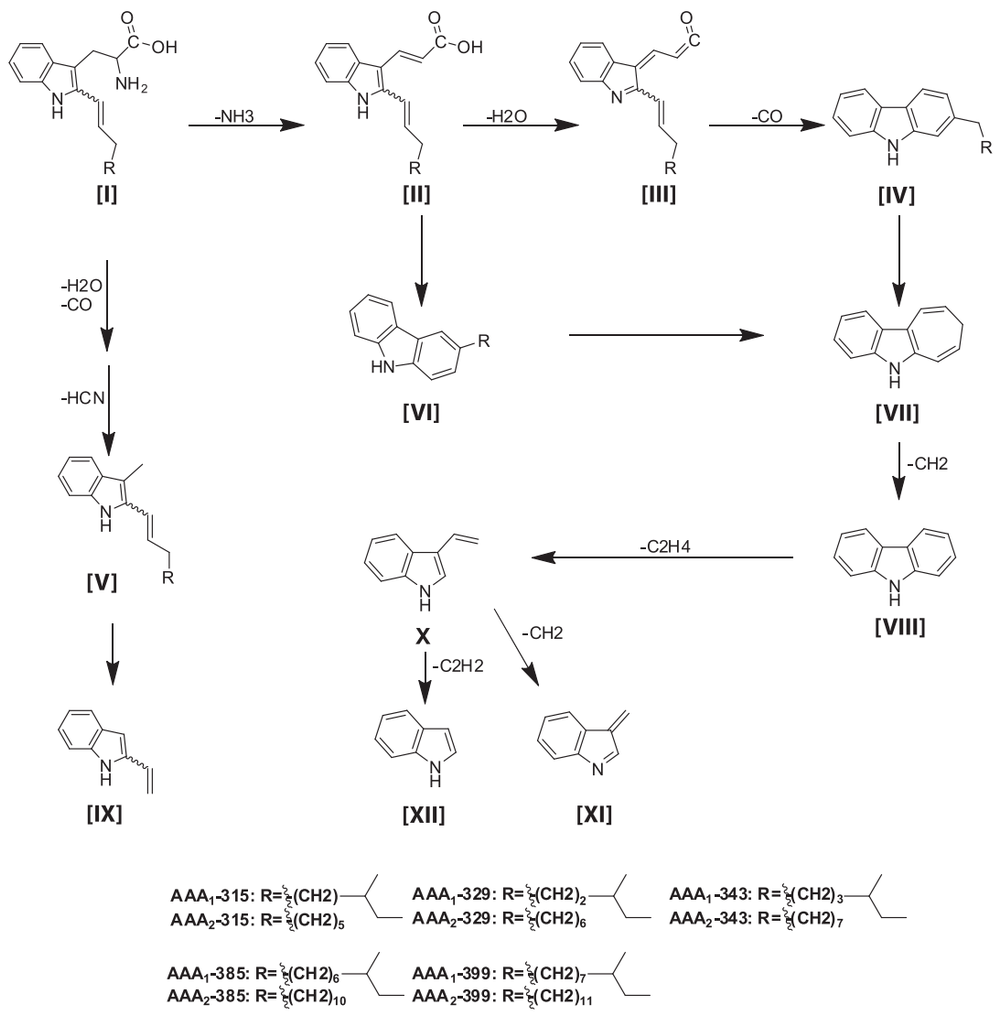

Scheme 1. Product ion mass spectral analysis of AAA_1-343/ AAA_2-343 as well as the AAA_1-XXX/AAA_2-XXX homolog ion species. Proposed product ion fragmentation pathways and structures based on MS/MS and MS^n analyses (Klarskov et al. 2018). The actual protonated molecular masses for individual ions are shown in Table 1 and 1S.

AAA_2-385 (*m/z* 308 and182) and AAA_1-399/AAA_2-399 (*m/z* 322 and 182) revealed that the same fragment ion losses (see Scheme 1,**[VI]** and **[VII]** respectively) occur for all the contaminants (see Fig. 4a-h, and Table 1 and Table S1). These MS/MS data for the product ions **[VI, VII,** and **VIII]** indicate that the aliphatic hydrocarbon chain is attached at the C-2 carbon of the indole ring. These data suggest that the ninth DoU is due to a double bond at the C1'-C2' position of the aliphatic chain. Only this regiochemistry and double bond location facilitates a energetically favoured intramolecular Diels-Alder ring formation (Demarque et al., 2016) of product ions **[II]** and **[III]** to afford the stable tricyclic ion at *m/z* 168 **[VIII]**, as well as the tricyclic product ions **[VI]** and **[VII]**, as seen in Scheme 1.

3.3.4. Aliphatic chain product ion series

The product ion spectra of AAA_1-343 and AAA_2-343 (Fig. 1a-b) and AAA_1-XXX/AAA_2-XXX Fig. 4a-h), all contained a low mass product ion series at *m/z* 57, and 43 which could either be protonated fragment ion (DoU = 1), or radical cations (DoU = 0) (see Table 1 and Table S1). It has been argued that such ions are typically produced by a charge-remote fragmentation process (Demarque et al., 2016), and are indicative of an aliphatic hydrocarbon chain often derived from a fatty acid (Murphy, 2015). The ion at *m/z* 43 indicates the presence of an *iso*-branched chain, and the ion at *m/z* 57 can indicate the presence of an *anteiso*-branched chain (Christie, 2017; Murphy, 2015; Ran-Ressler et al., 2011). However, these fragmentation processes are still poorly understood, and a multitude of mechanisms for such product ion formation have been postulated (Harvey, 2005; Murphy, 2015; Seto et al., 2001). Thus, this ion series clearly provides evidence that an aliphatic hydrocarbon chain is present in all eight AAA_1-XXX and AAA_2-XXX homologs (Klarskov et al., 2018). However, LC–MS/MS data alone were not sufficient to definitively identify the aliphatic chain isomers of the AAA_1-XXX and AAA_2-XXX compounds.

3.4. Aliphatic side chain isomer identification

We reported previously that AAA_1-343 was formed by the intermolecular condensation reaction of L-Trp with *anteiso* 7-methylnonanoic acid, and AAA_2-343 by the condensation reaction of L-Trp with *n*-decanoic acid. The *anteiso* to *linear* ratio was determined to be ~3:1 (Klarskov et al., 2018). These findings were predicated on the comparative analyses of HPLC retention times, accurate mass LC–MS, LC–MS/MS, and MS^n for AAA_1-343 and AAA_2-343 versus three synthetic standards, namely the *anteiso* isomer (*S*)-2-amino-3-(2-((*S,E*)-7-methylnon-1-en-1-yl)-1*H*-indol-3-yl)propanoicacid, *iso* isomer (*S*)-2-amino-3-(2((*E*)-8-methylnon-1-en-1-yl)-1*H*-indol-3-yl)propanoic acid, and *linear* isomer (*S*)-2-amino-3-(2-((*E*)-dec-1-en-1-yl)-1*H*-indol-3-yl) propanoicacid (Klarskov et al., 2018). Here we discuss the structure determination of the aliphatic chain isomer forms of AAA_1-XXX and AAA_2-XXX predicated on the original structure determination of AAA_1-343 and AAA_2-343.

3.4.1. MS/MS product ions

As described above the detection of a product ion at *m/z* 57 can indicate the specific presence of an *anteiso* aliphatic-branched chain (Christie, 2017; Murphy, 2015; Ran-Ressler et al., 2011). This ion was indeed detected in the MS/MS product ion spectrum of anteiso AAA_1-343 (Fig. 1a). The ratio of *m/z* 168 (MS/MS internal control ion) to *m/z* 57 was determined to be 49.4. However, inspection of the *linear* isomer AAA_2-343 (Fig. 1b) also revealed an ion at *m/z* 57, albeit at lower relative abundance with the ratio of *m/z* 168 to *m/z* 57 at 54.9. In the case of AAA_1-399 versus AAA_2-399 the relative ratio of *m/z* 168 to *m/z* 57 was 27.7-to-33.9 (Fig. 4g and h); AAA_1-385 versus AAA_2-385 was 35.8-to-41.6 (Fig. 4e and f); and for AAA_1-329 versus AAA_2-329 is 43.7-to-45.1 (Fig. 4c and d). In all four-ion pair cases the relative abundance of *m/z* 57 was higher in the AAA_1-343 and AAA_1-XXX series. These data support that the AAA_1 isomers of MH^+ 399, 385 and 329, are the *anteiso* chain isomers just like AAA_1-343. In the case of AAA_1-315 versus AAA_2-315 the ratio of *m/z* 168 to *m/z* 57 was 191.5/55.6 (Fig. 4a and b). This is due in part to the fact that no discernible fragment ion at *m/z* 57 was present for AAA_1-315 (Fig. 4a), and may be a consequence of the much shorter aliphatic chain length, which precludes a 1,4 elimination of the *anteiso* chain to afford this ion (Christie, 2017; Demarque et al., 2016; Murphy, 2015; Ran-Ressler et al., 2011).

3.4.2. HPLC relative retention times

The retention times of *anteiso* AAA_1-343 and *linear* AAA_2-343 utilizing a linear HPLC gradient differed by 0.19 min. at 2.49 min. and 2.68 min. respectively. (see Fig. 3c and Table 2). The HPLC retention time profile of synthetic AAA_x-343 isomers were *anteiso* < *iso* < *linear*, with retention time differences of 7.2% (0.18 min., *anteiso* v *linear*); 2.8% (0.06 min., *anteiso* v *iso*); and 4.3% (0.11 min., *iso* v *linear*) (Klarskov et al., 2018). The retention time difference for AAA_1-329 versus AAA_2-329 (Fig. 3b) and for AAA_1-315 versus AAA_2-315 (Fig. 3a) was almost identical to *anteiso* AAA_1-343 versus AAA_2-343 (Fig. 3c) at 0.19 min. and 0.18 min. respectively (Table 2). Based on this comparison with AAA_1-343/AAA_2-343 as well as the synthetic *anteiso*, *iso*, and *linear* standards, these isomer pairs AAA_1-329/AAA_2-329 and AAA_1-315/AAA_2-315 can only be the *anteiso* (AAA_1) and *linear* (AAA_2) isomers. In the case of the AAA_1-385/AAA_2-385 and AAA_1-399/AAA_2-399 ion pairs the HPLC retention time differences were slightly lower in value at 0.15 min and 0.14 min. respectively (Table 2). These data again indicate that each ion pair likely consists of the *anteiso* (AAA_1) and *linear* (AAA_2) isomers. However these latter retention time differences could also possibly indicate the presence of *iso* (AAA_1) and *linear* (AAA_2) isomer pairs predicated on the synthetic standards analysis (*iso* v *linear* difference, 0.11 min.) discussed above.

A number of studies have previously demonstrated that there is a linear correlation between increasing fatty acid aliphatic chain length and HPLC retention time in a homologous series (Brouwers et al., 1999; Smith and Jungalwala, 1981; Zhai and Reilly, 2002). Based on this consideration analyses of individual ion pair components and differences in aliphatic chain length were revealing (Table 2). The difference in retention times of AAA_1-343 versus AAA_1-329 versus AAA_1-315 was identical at (-) 0.4 min. (Table 2 and Fig. 3a-c). This reflects an iterative subtractive difference of a single methylene ($-CH_2$) group going from a C_{10} (AAA_1-343) to C_9 (AAA_1-329) to C_8 (AAA_1-315) aliphatic chain. This same identical trend was also observed for the difference in retention times of AAA_2-343 versus AAA_2-329 at 0.4 min. and AAA_2-329 versus AAA_2-315 at 0.41 min. (Table 2 and Fig. 3a-c). These data lead to the conclusion that the isomer pairs AAA_1-329/AAA_2-329 and AAA_1-315/AAA_2-315 can only be the *anteiso* (AAA_1) and *linear* (AAA_2) isomers.

The linear correlation of increased chain length versus increased relative retention time continued to hold for AAA_1-343/AAA_2-343 versus AAA_1-385/AAA_2-385 versus AAA_1-399/AAA_2-399 (Table 2 and Fig. 3c-e). In the case of AAA_1-385 an increased chain length of 3 x ($-CH_2$-) compared to AAA_1-343 should lead to a predicted retention time difference of 1.20 min., and the actual measured difference was 1.18 min. (Table 2, Fig. 3c and d). The observed retention time difference between AAA_1-385 and AAA_1-399 was 0.33 min (Table 2 and Fig. 3d and e) compared to the predicted of 0.4 min. However consideration of AAA_2-343 versus AAA_2-385 versus AAA_2-399 revealed very similar retention time differences of 1.14 min. and 0.32 min. respectively compared to the AAA_1 compounds (Table 2 and Fig. 3c-e). All these data are consistent with AAA_1-385/AAA_2-385 and AAA_1-399/AAA_2-399 also being the *anteiso* and *linear* isomer pairs.

3.5. Structure determination summary for fatty acid homologs

The presence of the prominent product ion at *m/z* 168 (Scheme 1 [**VIII**] in all fatty acid homologs (Fig. 4a-*h*) in combination with specific related product ions (Scheme 1 [**VI**] and [**VII**]) and analyses of other synthetic standards (discussed in detail elsewhere; Klarskov et al., 2018) indicates the position and stereoisomer form of the aliphatic side chain double bond. All these data are consistent with the aliphatic hydrocarbon chain being attached at the C-2 carbon of the indole ring in the trans (*E*) configuration. Only this regiochemistry and double bond location facilitates an energetically favored intramolecular Diels-Alder ring formation (Demarque et al., 2016) of product ions [**II**] and [**III**] to afford the stable tricyclic ion at *m/z* 168 [**VIII**], as well as the as the other tricyclic product ions [**IV**], [**VI**] and [**VII**]. This is all captured in Scheme 1.

The configuration of the chiral centers for AAA_1-343 and AAA_2-343 has been discussed in detail elsewhere (Klarskov et al., 2018). The same considerations can be applied to the AAA_1-XXX and AAA_2-XXX family members. Briefly, SD genetically engineered *Bacillus amyloliquefaciens* to produce exclusively L-Trp (Akashiba et al., 1982). Hence the absolute configuration of the amino-containing α-carbon can be assigned as (*S*). In addition, it has been reported that in the case of *Bacillus* sp. that produce *anteiso* fatty acids the chiral carbon containing the branched methyl group is always in the (*S*) configuration (Hauff et al., 2010; Christie, 2017). Therefore we postulate that for all of the fatty acid homolog AAA_1-XXX series the chiral centers are both (*S*), and for the AAA_2-XXX series the amino-containing α-carbon is also (*S*).

The structure determination of an unknown(s) is a complicated process. Dias and colleagues in their recent paper have argued, "MS alone is not able to unambiguously identify a molecule and must rely on complementary sources of information (e.g., chromatographic retention time, or MS/MS,) (Dias et al., 2016). Accordingly, the following guidelines for structure determination of metabolites and other small molecules have been met and are as follows:

1 "Confident identifications are based upon a minimum of two

Table 2
HPLC Retention time differences of AAA_1-XXX and AAA_2-XXX contaminants.

AAA Member	Retention Time (min) 315	329	343	385	399
1	1.69	2.09	2.49	3.67	4.00
2	1.87	2.28	2.68	3.82	4.14
ΔRT	0.18	0.19	0.19	0.15	0.14
ΔRT (min) 1	0.40	0.40	1.18	0.33	
ΔRT (min) 2	0.41	0.40	1.14	0.32	

different pieces of confirmatory data relative to an authentic standard." We have provided three such confirmatory data sets relative to characterized synthetic standards. They include accurate mass MS, accurate mass MS/MS and MS^n, and LC–MS retention time data.

2 "Putatively annotated compounds and putatively characterized compound classes" should be compared to the metabolite or other small molecule We have discussed in detail the MS/MS spectra of authentic SD L-Trp derived AAA_1-343 and AAA_2-343 and compared and contrasted these data to that published in the literature/databases for component elements of these contaminants.

Subsequently, we compared the HPLC retention times, accurate mass MS, accurate mass LC–MS and accurate mass MS/MS datasets of AAA_1-XXX and AAA_2-XXX homologs to both synthetic and SD L-Trp derived AAA_1-343 and AAA_2-343. Consideration of all of these elements satisfy the current criteria for the structure determination of, in this case, the fatty acid L-Trp homolog contaminants found in SD L-Trp. These contaminants have been identified as (*S*)-2-amino-3-(2-((*S,E*)-5-methylhept-1-en-1-yl)-1*H*-indol-3-yl)propanoic acid (AAA_1-315); (*S*)-2-amino-3-(2-((*E*)-oct-1-en-1-yl)-1*H*-indol-3-yl)propanoic acid (AAA_2-315); (*S*)-2-amino-3-(2-((*S,E*)-6-methyloct-1-en-1-yl)-1*H*-indol-3-yl) propanoic acid (AAA_1-329); (*S*)-2-amino-3-(2-((*E*)-non-1-en-1-yl)-1*H*-indol-3-yl)propanoic acid (AAA_2-329); (*S*)-2-amino-3-(2-((*S,E*)-10-methyldodec-1-en-1-yl)-1*H*-indol-3-yl)propanoic acid (AAA_1-385); (*S*)-2-amino-3-(2-((*E*)-tridec-1-en-1-yl)-1*H*-indol-3-yl)propanoic acid (AAA_2-385); (*S*)-2-amino-3-(2-((*S,E*)-11-methyltridec-1-en-1-yl)-1*H*-indol-3-yl) propanoic acid (AAA_1-399); and (*S*)-2-amino-3-(2-((*E*)-tetradec-1-en-1-yl)-1*H*-indol-3-yl)propanoic acid (AAA_2-399). All these structures are shown in Fig. 5.

3.6. Quantification of AAA_1-XXX and AAA_2-XXX contaminants

Prior to the EMS outbreak, L-Trp was perceived as a safe, and effective dietary supplement. As such, individuals self-medicated and typically used L-Trp for insomnia, depression and premenstrual syndrome (UK Committee on Toxicology (COT, 2004). Individuals in the UK usually ingested 1–2 tablets or capsules containing 500 mg of L-Trp per unit dose (UK Committee on Toxicology (COT, 2004). Daily intake in the USA was more variable and ranged from ~500 mg- > 4000 mg per day (Henning et al., 1993; Vierk, 2018). Kamb suggested that among patients taking > 4000 mg of SD L-Trp "the definite EMS attack rate was 59% and the pooled attack rate (definite and possible EMS) was 84%" (Kamb et al., 1992). Belongia supported these findings by suggesting, "that exposure to higher doses of L-Trp may have contributed to the pathogenesis of EMS", and that a "dose-response relationship" had been observed between SD L-Trp ingested and EMS onset (Belongia, 2004). Since dose was potentially related to EMS onset, we determined the amounts of AAA_1-XXX and AAA_2-XXX contaminants present in SD L-Trp.

Initially we determined the amount of AAA_1-343 present in SD L-Trp employing synthetic AAA_1-343 to create a calibration curve as described in the Materials and Methods Section 2.4.2. We then used the relative ion counts from Fig. 3, to determine the relative ratios (%) of the remaining AAA_1-XXX and AAA_2-XXX contaminants. The relative ratios were then used to estimate the amount of the other AAA_1-XXX/AAA_2-XXX contaminants present in SD L-Trp. This is all summarized in Table 3. It should be noted that the concentration values shown in Table 3 assumes that the ionization potential of each AAA_1-XXX/AAA_2-XXX compound is approximately the same, and is not significantly affected by varying the fatty acid-derived chain lengths of each contaminant. Furthermore, the values in Table 3 do not take into account a potential loss of contaminants during the pre-analytic purification solid phase extraction, hence may be an under-estimation of the actual amounts. The relative ratios (%) revealed that the three medium chain length contaminants AAA_1-329, AAA_1-343 and AAA_1-315, were the most abundant compounds present in SD L-Trp. The long chain contaminants AAA_1-399 and AAA_1-385 were present at much smaller amounts. Perusal of Table 3 reveals that individuals consuming a single 500 mg SD L-Trp tablet/capsule per day would be exposed to ~0.1–7.9 μg of each contaminant. However, for patients ingesting 4000 mg of SD L-Trp, the amount of AAA_1-XXX/AAA_2-XXX consumed would be ~ 0.8–63.2 μg per day.

Table 3
Quantification of AAA_1-XXX and AAA_2-XXX contaminants.

AAA Isomer	Relative Ratio (%)[a]	Concentration (μg/500 mg)[b,c]	Concentration (μg/4000 mg)[d]
AAA_1-329	100.0	7.9	63.2
AAA_2-329	33.0	2.7	21.6
AAA_1-343	49.0	3.9	31.2
AAA_2-343	20.0	1.6	12.8
AAA_1-315	7.0	0.6	4.8
AAA_2-315	2.5	0.2	1.6
AAA_1-399	3.0	0.3	2.4
AAA_2-399	1.0	0.1	0.8
AAA_1-385	1.5	0.2	1.6
AAA_2-385	1.0	0.1	0.8

[a] AAA_1-329 was the most abundant ion and was arbitrarily assigned a value of 100%. All other relative ion abundances are reported as a % of AAA_1-329.

[b] Only AAA_1-343 was actually quantified using synthetic standard AAA_1-343 to construct a calibration curve. All other concentrations were based on the relative ion abundance raw data used in Fig. 3.

[c] A typical daily dose of SD L-Trp consisted of a 500 mg tablet or capsule.

[d] A daily dose of 4000 mg or more of SD L-Trp was associated with a higher probability of EMS onset (Kamb et al., 1992).

3.7. Structural similarities of EMS versus TOS contaminants

Kilbourne and coworkers have described the striking similarity of EMS and TOS clinical symptoms (Kilbourne et al., 1991). In particular, both patient groups manifested intense peripheral eosinophilia.

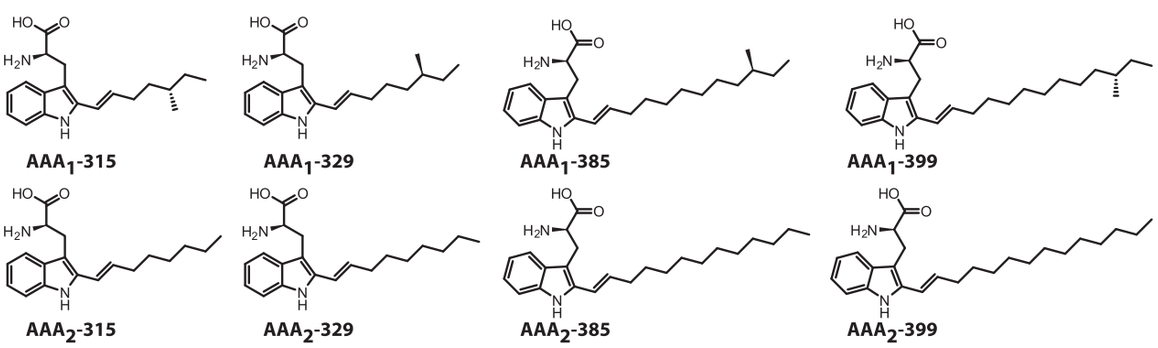

Fig. 5. Structures of the fatty acid homolog SD L-Trp contaminants.
AAA_1-315, AAA_2-315, AAA_1-329, AAA_2-329, AAA_1-385, AAA_2-385, AAA_1-399, and AAA_2-399.

Kilbourne has noted that in TOS, “Virtually all patients had absolute eosinophil counts > 500 cells/mm^3, but counts of > 2000 cells/mm^3 were common, in contrast to normal levels in healthy humans of 50–350 cells/mm^3. Eosinophilia was so frequent as to be considered a hallmark of the disease”. He noted also that “Patients with EMS typically come [*sic*] to medical attention because of persistent and severe myalgia, much like that associated with intermediate and chronic- and to some extent in acute-TOS. The eosinophil count is dramatically increased, usually > 2000 cells/mm^3” (Kilbourne et al., 1991). In addition there were numerous other common symptoms that included liver enzyme elevation, selective inflammation of intramuscular nerve and muscle spindles, axonal neuropathy and severe myalgia (Gelpi et al., 2002; Kilbourne et al., 1991).

Common symptomology often indicates a shared etiology of different disease states (Naylor and Chen, 2010). We have argued previously that there may be a common causal contaminant(s) since both TOS and EMS onset appeared to have strong associations with ingested, contaminated food (oil; TOS) and dietary supplement (L-Trp; EMS) (Mayeno et al., 1995). Aniline contaminants, including 3-(phenylamino)-1,2-propanediol (PAP), have been identified in the adulterated oil used by patients who developed TOS. A related aniline derivative, PAA was identified as a case-associated contaminant isolated from SD L-tryptophan associated with the onset of EMS. We demonstrated that it was possible to bio-transform PAP into PAA using both rat hepatocytes and human liver tissue. Our stated conclusions were, that “this finding is the first reported chemical link between TOS and EMS and suggests that these two related diseases share a common etiology, namely, PAA” (Mayeno et al., 1995).

The structure determination of AAA_1-343/AAA_2-343 and AAA_1-XXX/AAA_2-XXX has revealed a family of closely related L-Trp aliphatic chain condensation products. It is noteworthy that during the 1990′s reanalyses of toxic oil contaminants using LC–MS/MS revealed a number of “new” compounds “associated with the risk of disease”. The contaminants were identified as fatty acid esters of PAP, namely the 1-oleyl-ester (O-PAP) and 1,2-di-oleyl ester (OO-PAP). These structures are shown in Fig. 6 (Gelpi et al., 2002). O-PAP, OO-PAP and the AAA family members share structural features, i.e. an electron-rich aromatic ring connected to an unsaturated aliphatic chain, which may suggest they share similar absorption, distribution, metabolism, and excretion pathways upon ingestion. These structural similarities raise the intriguing prospect that it may actually be metabolites of these case-associated contaminants that caused EMS or TOS onset. This consideration has rarely, if ever been addressed. Our work and others have been primarily focused on the structure determination of the actual contaminants (Goda et al., 1992; Muller et al., 1991; Mayeno et al., 1990; Mayeno et al., 1992; Smith et al., 1991; Williamson et al.,1997; Williamson et al., 1998b). More recently we have noted the importance of such a possibility and suggest this warrents more consideration using appropriate animal models (Naylor, 2017).

4. Conclusions

We have determined the structures of eight new members of the AAA family of contaminants present in SD L-Trp. All eight compounds are structural homologs of AAA_1-343 and AAA_2-343. Hill and coworkers described previously that “Peak AAA” was the most statistically significant contaminant in terms of association with EMS cases (Hill et al., 1993; Philen et al., 1993). It is however unclear at the moment whether these structural homologs may have contributed to the causal onset of EMS in patients who ingested SD L-Trp. But it is noteworthy that such compounds are lipid soluble and hence may result in bioaccumulation in adipose tissue. However the structural similarities of the AAA family to the TOS case- related contaminants O-PAP and OO-PAP are intriguing. We suggest that this is the second example of commonality between case associated contaminants in both TOS oil and EMS L-Trp.

Prostaglandin D_2 is a major mast cell mediator and a potent eosinophil chemo-attractant and is thought to be involved in eosinophil recruitment to sites of allergic inflammation (Hirai et al., 2001). The presence of unsaturated aliphatic chains in Prostaglandin D_2 and its role in eosinophil chemotaxis lends some support to the fact that such a presence, in the AAA family and O-PAP/OO-PAP may play a role in eosinophil recruitment. These consistent structural homologies may afford opportunity to further elaborate the possible etiological role of the AAA family in the causal onset of EMS in patients that consumed SD L-Trp.

Conflict of interests

None

Transparency document

The Transparency document associated with this article can be found in the online version.

Acknowledgements

SN and GJG thank Mayo Foundation and NIH (Grant AI-31155) for funding the original work carried out at Mayo Clinic. KK acknowledges the Natural Sciences and Engineering Research Council of Canada (NSERC-Grant RGPIN-2014-04234) and KK and EM thank the Centre de Proteomique Structurale et Fonctionnelle des Proteomes (University of Sherbrooke) for a pilot project grant. We also thank Ms. Lois Vierk (President) and Members of the National Eosinophilia Myalgia Syndrome Network (http://www.nemsn.org) for their help in

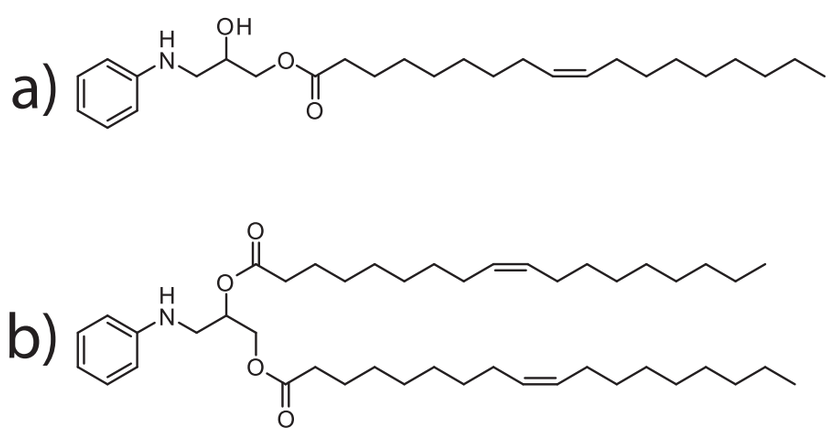

Fig. 6. Structures of TOS contaminants associated with risk of disease; a) O-PAP b) OO-PAP.

determining the L-Trp doses taken by patients up to, and during the original EMS outbreak.

Appendix A. Supplementary data

Supplementary material related to this article can be found, in the online version, at doi:https://doi.org/10.1016/j.toxlet.2018.05.027.

References

Akashiba, T., Nakayama, A. and Murata, A. (1982). Process for Producing L- Tryptophan, A Pure Culture of a Microorganism Strain used in Said Process. USA Patent 4,363, 875. December 14th, 1982.

Belongia, E.A., Hedberg, C.W., Gleich, G.J., White, K.E., Mayeno, A.N., Loegering, D.A., et al., 1990. An investigation of the cause of the eosinophilia-myalgia syndrome associated with tryptophan use. N. Engl. J. Med. 323, 357–365.

Belongia, E.A., Mayeno, A.N., Osterholm, M.T., 1992. The eosinophilia myalgia syndrome and tryptophan. Annu. Rev. Nutr. 12, 235–256.

Belongia, E., 2004. Toxic tryptophan? Investigating the eosinophilia-myalgia syndrome in Minnesota. In: Dworkin, M.S. (Ed.), Cases in Field Epidemiology: A Global Perspective. Jones & Barlett Learning, Sudbury, NA, USA, pp. 313–337 Chapter 26.

Brouwers, J.F.H.M., Vernooij, E.A.A.M., Tielens, A.G.M., van Golde, L.M.G., 1999. Rapid separation and identification of phosphatidylethanolamine molecular species. J. Lipid Res. 40, 164–169.

Christie, W.W., 2017. Lipid Web: Saturated Branched-Chain Fatty Acids. http://www.lipidhome.co.uk/ms/methesters/me-0dbbr/index.htm.

Demarque, D.P., Crotti, A.E.M., Vessecchi, R., Lopes, J.L.C., Lopes, N.P., 2016. Fragmentation reactions using electrospray ionization mass spectrometry: an important tool for the structural elucidation and characterization of synthetic and natural products. Nat. Prod. Rep. 33, 432–455.

Dias, D.A., Jones, O.A.H., Beale, D.J., Boughton, B.A., Benheim, D., Kouremenos, K.A., et al., 2016. Current and future perspectives on the structural identification of small molecules in biological systems. Metabolites 6, 46–57.

Eidson, M., Philen, R.M., Sewell, C.M., Voorhees, R., Kilbourne, E.M., 1990. L-tryptophan and eosinophilia-myalgia syndrome in New Mexico. Lancet 335, 645–648.

El Aribi, H., Orlova, G., Hopkinson, A.C., Siu, K.W.M., 2004. Gas-phase fragmentation reactions of protonated aromatic amino acids: concomitant and consecutive neutral eliminations and radical cation formations. J. Phys. Chem. A 108, 3844–3853.

Gelpi, E., Posada de la Paz, M., Terracini, B., Abaitua, I., Gomez de la Paz, A., Kilbourne, E.M., et al., 2002. The Spanish toxic oil syndrome 20 years after its onset: a multidisciplinary review of scientific knowledge. Environ. Health Perspect. 5, 457–463.

Glish, G.L., Vachet, R.W., 2003. The basics of mass spectrometry in the twenty-first century. Nat. Rev. Drug Discov. 2, 140–150.

Goda, Y., Suzuki, J., Maitani, T., Yoshihira, K., Takeda, M., Uchiyama, M., 1992. 3-anilino-L-alanine, structural determination of UV-5, a contaminant in EMS-associated L-tryptophan samples. Chem. Pharm. Bull. (Tokyo) 40, 2236–2238.

Gross, B., Ronen, N., Honigman, S., Livne, E., 1999. Tryptophan toxicity-time and dose response in rats. Adv. Expt. Med. Biol. 467, 507–516.

Harvey, D.J., 2005. A New charge-associated mechanism to account for the production of fragment ions in the High-energy CID spectra of fatty acids. J. Am. Soc. Mass Spectrom. 16, 280–290.

Hauff, S., Rilfors, L., Hottinger, G., Vetter, W., 2010. Structure and absolute configuration of an unsaturated anteiso fatty acid from bacillus megaterium. J. Chromatogr. A 1217, 1683–1687.

Henning, K.J., Jean-Baptiste, E., Singh, T., Hill, R.J., Friedman, S.M., 1993. Eosinophilia-myalgia syndrome in patients ingesting a single source of L-tryptophan. J. Rheumatol. 20, 273–278.

Hertzman, P.A., Falk, H., Kilbourne, E.M., Page, S., Shulman, L.E., 1991. The eosinophilia-myalgia syndrome: the Los alamos conference. J. Rheumatol. 18, 867–873.

Hertzman, P.A., Clauw, D.J., Duffy, J., Medsger Jr., T.A., Feinstein, A.R., 2001. Rigorous New approach to constructing a Gold standard for validating New diagnostic criteria, as exemplified by the eosinophilia-myalgia syndrome. Arch. Intern. Med. 161, 2301–2306.

Hill Jr., R.H., Caudill, S.P., Philen, R.M., Bailey, S.L., Flanders, W.D., Driskell, W., et al., 1993. Contaminants in L-tryptophan associated with eosinophilia- myalgia syndrome. Arch. Environ. Contam. Toxicol. 25, 134–142.

Hirai, H., Tanaka, K., Yoshie, O., Ogawa, K., Kenmotsu, K., Takamori, Y., et al., 2001. Prostaglandin D2 selectively induces chemotaxis in t helper type 2 cells, eosinophils, and basophils via seven-transmembrane receptor Crth2. J. Exp. Med. 193, 255–262.

Kamb, M.L., Murphy, J.J., Jones, J.L., Caston, J.C., Nederlof, K., Horney, L.F., et al., 1992. Eosinophilia-myalgia syndrome in L-tryptophan-exposed patients. JAMA 267, 77–82.

Kilbourne, E.M., Posada de la Paz, M., Borda, I.B., Ruiz-Navarro, M.D., Philen, R.M., Falk, H., 1991. Toxic oil syndrome: a current clinical and epidemiologic summary, including comparisons with the eosinophilia-myalgia syndrome. J. Am. Coll. Cardiol. 18, 711–717.

Kilbourne, E.M., 1992. Eosinophilia-myalgia syndrome: coming to grips with a New illness. Epidemiol. Rev. 14, 16–36.

Klarskov, K., Johnson, K.L., Gleich, G.J., Naylor, S., 2000. Structural of a contaminant in L-tryptophan associated with eosinophilia-myalgia syndrome Long Beach, California, USA. 48Th American Society for Mass Spectrometry and Allied Topics Meeting, June 11-15Th, 2000.

Klarskov, K., Gagnon, H., Boudreault, P.-L., Normandin, C., Plancq, B., Marsault, E., et al., 2018. Structure determination of disease associated Peak AAA from L- tryptophan implicated in the eosinophilia-myalgia syndrome. Toxicol. Lett. 282, 71–80.

Lioe, H., O'Hair, R.A., Reid, G.E., 2004. Gas-phase reactions of protonated tryptophan. J. Am. Soc. Mass Spectrom. 15, 65–76.

Martin, R.W., Duffy, J., Engel, A.G., Lie, J.T., Bowles, C.A., Moyer, T.P., Gleich, G.J., 1990. The clinical spectrum of the eosinophilia-myalgia syndrome associated with L-tryptophan ingestion. Clinical features in 20 patients and aspects of pathophysiology. Ann. Intern. Med. 113, 124–134.

Mayeno, A.N., Lin, F., Foote, C.S., Loegering, D.A., Ames, M.M., Hedberg, C.W., Gleich, G.J., 1990. Characterization of 'Peak E', a novel amino acid associated with eosinophilia-myalgia syndrome. Science 250, 1707–1708.

Mayeno, A.N., Belongia, E.A., Lin, F., Lundy, S.K., Gleich, G.J., 1992. 3-(phenylamino) alanine, a novel aniline-derived amino acid associated with the eosinophilia-myalagia syndrome: a link to the toxic oil syndrome? Mayo Clin. Proc. 67, 1134–1139.

Mayeno, A.N., Gleich, G.J., 1994. The eosinophilia-myalgia syndrome and tryptophan production: a cautionary tale. Trends Biotechnol. 12, 346–352.

Mayeno, A.N., Benson, L.M., Naylor, S., Colberg-Beers, M., Puchalski, J.T., Gleich, G.J., 1995. Biotransformation of 3-(phenylamino)-1,2-propanediol to 3- (phenylamino) alanine: a chemical link between toxic oil syndrome and eosinophilia-myalgia syndrome. Chem. Res. Toxicol. 8, 911–916.

Muller, A., Busker, E., Gunther, K., Hoppe, B., 1991. Characterization of By-products in L-Tryptophan. Bioforum 14, 350–354.

Murphy, R.C., 2015. Tandem Mass Spectrometry of Lipids: Molecular Analysis of Complex Lipids. Cambridge, UK. .

Naylor, S., Chen, J.Y., 2010. Unraveling human complexity and disease with systems biology and personalized medicine. Pers. Med. 7, 275–289.

Naylor, S., 2017. Eosinophilia myalgia syndrome contaminants: past, present, future. National Eosinophilia-Myalgia Syndrome Network; December 2017 Newsletter. . http://www.nemsn.org/sites/default/files/newsletters/NEMSN-2017Dec.pdf.

Noakes, R., Spelman, L., Williamson, R., 2006. Is the L-tryptophan metabolite quinolinic acid responsible for eosinophilic fasciitis? Clin. Exp. Med. 6, 60–64.

Oberacher, H., 2013. Applying tandem mass spectral libraries for solving the critical assessment of small molecule identification (CASMI) LC/MS challenge 2012. Metabolites 3, 312–324.

Philen, R.M., Hill Jr., R.H., Flanders, W.D., Caudill, S.P., Needham, L., Sewell, L., et al., 1993. Tryptophan contaminants associated with eosinophilia-myalgia syndrome. Am. J. Epidemiol. 138, 154–159.

Ran-Ressler, R.R., Lawrence, P., Brenna, J.T., 2011. Structural characterization of saturated branched chain fatty acid methyl esters by collisional dissociation of molecular ions generated by electron ionization. J. Lipid Res. 53, 195–203.

Seto, C., Grossert, J.S., Waddell, D.S., Curtis, J.M., Boyd, R.K., 2001. Effects of ionization Mode on charge-site- remote and related fragmentation reactions of Long-Chain quaternary ammonium ions. J. Am. Soc. Mass Spectrom. 12, 571–579.

Simat, T.J., Kleeberg, K.K., Muller, B., Sierts, A., 1999. Synthesis, formation and occurrence of contaminants in biotechnologically manufactured L- tryptophan. In: Huether, G., Kochen, W., Simat, T.J., Steinhart (Eds.), Tryptophan, Serotonin, and Melatonin: Basic Aspects and Applications, pp. 469–480 Adv. Expt. Med. Biol. 467.

Slutsker, L., Hoesly, F.C., Miller, L., Williams, L.P., Watson, J.C., Fleming, D.W., 1990. Eosinophilia-myalgia syndrome associated with exposure to tryptophan from a single manufacturer. J. Am. Med. Assoc. 264, 213–217.

Smith, M., Jungalwala, F.B., 1981. Reversed-phase High performance liquid chromatography of phosphatidylcholine: a simple method for determining relative hydrophobic interact- ion of various molecular species. J. Lipid Res. 22, 697–704.

Smith, M.J., Mazzola, E.P., Farrel, T.J., Sphon, J.A., Page, S.W., Ashley, D., et al., 1991. 1,1'-ethyl-idenebis(L-tryptophan), structure determination of contaminant '97'-implicated in the eosinophilia-myalgia syndrome (EMS). Tetrahedron. Lett. 32, 991–994.

Smith, M.J., Garrett, R.H., 2005. A heretofore-undisclosed crux of eosinophilia-myalgia syndrome: compromised histamine degradation. Inflamm. Res. 54, 435–450.

Swygert, L.A., Maes, E.F., Sewell, L.E., Miller, L., Falk, H., Kilbourne, E.M., 1990. Eosinophilia-myalgia syndrome: results of national surveillance. J. Am. Med. Assoc. 264, 1698–1703.

Swygert, L.A., Back, E.E., Auerbach, S.B., Sewell, L.E., Falk, H., 1993. Eosinophilia-myalgia syndrome: mortality data from the US national surveillance system. J. Rheumatol. 20, 1711–1717.

Toyo'oka, T., Yamazaki, T., Tanimoto, T., Sato, K., Sato, M., Toyoda, M., et al., 1991. Characterization of contaminants in EMS-associated L-tryptophan samples by High performance liquid chromatography. Chem. Pharm. Bull. 39, 820–822.

Trucksess, M.W., 1993. Separation and isolation of trace impurities in L- tryptophan by High performance liquid chromatography. J. Chromatogr. 630, 147–150.

UK Committee on Toxicology (COT), 2004. COT Statement on Tryptophan and the Eosinophilia-Myalgia Syndrome, Committee on the Toxicity of Chemicals in Food, Consumer Products and the Environment, United Kingdom. https://cot.food.gov.uk/sites/default/files/cot/tryptophanamend200401.pdf.

Vierk, L., 2018. Personal Communication That Included Discussions With Patients/ Board Members of the National Eosinophilia-Myalgia Syndrome Network (NEMSN-. http://www.nemsn.org.

Williamson, B.L., Benson, L.M., Tomlinson, A.J., Mayeno, A.N., Gleich, G.J., Naylor, S., 1997. On-line HPLC tandem mass spectrometry analysis of contaminants of L-tryptophan associated with the onset of the eosinophilia- myalgia syndrome. Toxicol. Lett. 92, 139–148.

Williamson, B.L., Tomlinson, A.J., Hurth, K.M., Posada de la Paz, M., Gleich, G.J., Naylor, S., 1998a. Rapid HPLC screening method for contaminants found in implicated L-tryptophan associated with eosinophilia myalgia syndrome and adulterated rapeseed oil associated with toxic oil syndrome. Biomed. Chromatogr. 12, 255–261.

Williamson, B.L., Johnson, K.L., Tomlinson, A.J., Gleich, G.J., Naylor, S., 1998b. On-line HPLC tandem mass spectrometry structural characterization of case-associated contaminants of L-tryptophan implicated with the onset of eosinophilia-myalgia syndrome. Toxicol. Lett. 99, 139–150.

Zhai, D., Reilly, P.J., 2002. Effect of fatty acid Chain length on Normal- and reversed-phase HPLC of phospholipids. J. Am. Oil Chem. Soc. 79, 1187–1190.